

Systematic Development of Nonlinear Analog Circuit Macromodels through Successive Operator Composition and Nonlinear Model Decoupling

Ying Wei, Alex Doboli

Department of Electrical and Computer Engineering,
Stony Brook University, Stony Brook, NY, 11794-2350

ywei,adoboli@ece.sunysb.edu

ABSTRACT

This paper presents a systematic methodology for developing structural nonlinear macromodels for analog circuits. The methodology includes two steps: first, a nonlinear system is represented as a system with nonlinear inputs and linearly coupled blocks. Then, the linear couplings are removed. The methodology also uses a novel description of circuit nonlinearities as a successive composition of three operators. The generated nonlinear models are scalable, tunable according to the required accuracy, and offer insight into the circuit operation.

Categories and Subject Descriptors

I.6.5 [Model Development]: Modeling methodologies

General Terms

Algorithms, Design

Keywords

Analog circuits, Structural macromodel, Nonlinear macromodel

1. INTRODUCTION

Circuit linearity is one of the most important design specifications for analog and mixed-signal circuits, as it limits the dynamic range of a system [7, 8]. The overall circuit linearity is usually evaluated by detailed circuit simulation. However, simulation has two main drawbacks: (1) insight into circuit operation and performance tradeoffs is difficult to acquire, and (2) time-domain simulation is time consuming and has often poor convergency. These limitations can be tackled by developing compact macromodels for capturing the nonlinear behavior of a circuit. Nevertheless, macromodeling is challenging because of the complexity of representing and understanding the nonlinear behavior of strongly coupled devices in an analog circuit.

Modeling of the nonlinear behavior of analog circuits is largely an unsolved problem. Existing nonlinear modeling approaches are grouped into two main categories: (1) analytical methods, e.g., Volterra series based [7], perturbation analysis [9], and root localization [5], and (2) simulation-based methods, such as per-nonline-

Permission to make digital or hard copies of all or part of this work for personal or classroom use is granted without fee provided that copies are not made or distributed for profit or commercial advantage and that copies bear this notice and the full citation on the first page. To copy otherwise, to republish, to post on servers or to redistribute to lists, requires prior specific permission and/or a fee.

DAC 2006, July 24–28, 2006, San Francisco, California, USA.

Copyright 2006 ACM 1-59593-381-6/06/0007 ...\$5.00.

arity method [3] and piecewise approximation [1, 4]. In addition, model order reduction techniques are employed to reduce the complexity of the modeling space [2, 10]. Analytical methods have the advantage of computing symbolic expressions for the nonlinear circuit performance, and thus offer some limited description of the distortion generating mechanism. However, analytical techniques mostly produce blackbox models that are just mathematical equivalents of a circuit, without offering insight into the physical meaning of the circuit operation and performance tradeoffs. New methods are needed for structural nonlinear macromodeling.

This paper presents a systematic methodology to create structural nonlinear macromodels customized for a specific analog circuit. The idea is to approximate a nonlinear system as a system with nonlinear inputs and linear dependencies of its composing blocks. Then, the linear dependencies are removed through uncoupling to get the structural macromodel of a circuit. The proposed nonlinear macromodeling technique incorporates three novel contributions: (1) a new description format for circuit nonlinearities. The format is highly regular, and is based on successive composition of three operators (called F , G , and H). (2) A nonlinear decoupling algorithm that uses the operator based description to approximate higher order nonlinear dependencies by lower order nonlinear dependencies and nonlinear transformation of the inputs, and (3) an iterative algorithm that automatically generates the equivalent nonlinear current sources according to the desired modeling accuracy.

Produced macromodels capture the circuit distortion by symbolically characterized nonlinear current sources. Models are structural, thus each of their composing elements has a physical interpretation in terms of the original circuit. In addition, macromodels are scalable, and their accuracy is controllable. Experiments showed that models have good prediction accuracy compared to SPICE simulation. The method requires a low modeling effort, as there is little designer input or data sampling required. In addition, there are several other advantages compared to existing nonlinear modeling approaches. Unlike Volterra-based methods [7], which require separate models to capture different orders of distortion, our technique produces an integrated nonlinear model that captures all circuit nonlinearities of different orders. Also, as opposed to the per-nonlinearity method [3], the suggested technique provides fine distortion diagnosis about the contribution from a particular nonlinearity, and does not require iterative simulation of the circuit.

The paper has the following structure. Section 2 summarizes related work. Section 3 presents the transformation algorithm to describe MOSFET nonlinearities. Section 4 introduces the nonlinear decoupling algorithm. Section 5 discusses experimental results for two analog circuits. Finally, conclusions are offered.

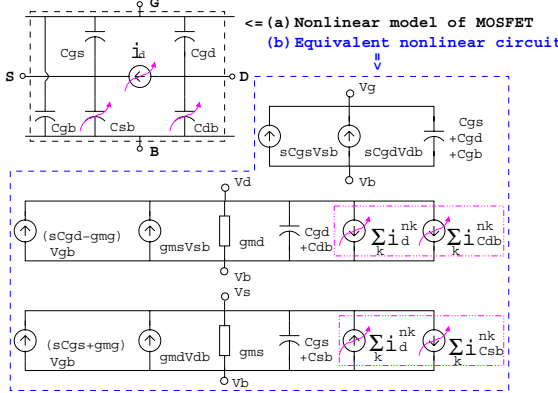


Figure 1: Nonlinear model of a MOSFET transistor

2. RELATED WORK

Volterra-based methods [6, 7] are widely used for distortion analysis. The produced behavioral models predict the dominant nonlinear effects using a composition of linear transfer functions and multiplications. However, this method is only suitable for frequency domain analysis of weakly nonlinear circuit, and the modeling complexity grows exponentially with the number of nonlinear components in the circuit. Perturbation-based nonlinear distortion analysis [9] is an alternative to Volterra series methods. Unlike Volterra series, this method can be applied to nonlinearities of any type, given that the Fourier coefficients of periodic functions are calculated in a closed form (i.e., polynomial, exponential, and so on). Li and Pileggi [2, 3] suggest linear-centric circuit models to generate the individual distortion contributions of each nonlinear component in a circuit. The method is simpler and more efficient than Volterra series based approaches. However, linear-centric models cannot distinguish the contributions from the different nonlinear coefficients of a nonlinear element, which Volterra series can do. PWP approach [1] approximates a nonlinear system as piecewise polynomials (PWP) over a number of regions, followed by reducing the model of each region via polynomial model reduction. Model order reduction (MOR) techniques have been used to reduce the modeling space [2, 11]. The major problem is that the techniques are either applicable to only weakly nonlinear systems, or they work only for some input signals close to some special training input, which was used during model extraction. Moreover, produced models are just mathematical equivalents of the original circuit, are basically uninterpretable, and have poor reusability.

To conclude, present circuit modeling methods are mostly for blackbox modeling in the frequency-domain. There are few systematic techniques for creating structural nonlinear macromodels that offer insight into the circuit operation without requiring iterative excitation of the circuit.

3. DESCRIPTION OF NONLINEARITIES

This section summarizes the nonlinear model of a MOS transistor based on power series. Then, it proposes a transformation algorithm for deriving the nonlinearity of a MOS transistor by iteratively composing three linear operators (called operators F , G , and H) on the terminal voltages.

3.1 Preliminaries on MOSFET modeling using Volterra series

Figure 1 presents the nonlinear model of a MOS transistor with the bulk as a reference. The model has three nonlinear elements, the drain current i_D , and capacitors C_{sb} and C_{db} . This nonlinear equivalent circuit for a MOS transistor is valid for low and medium-

high frequencies, typically up to a tenth of the cutoff frequency [8].

The nonlinear elements can be described by power series. Capacitors C_{sb} and C_{db} are modeled as voltage controlled current sources depending on the voltages v_{sb} and v_{db} . The power series for the capacitors can be expressed as [8]:

$$\begin{aligned} i_{C_{sb}} &= \frac{d}{dt} (C_{sb}v_{sb} + K_{2C_{sb}}v_{sb}^2 + K_{3C_{sb}}v_{sb}^3 + \dots) \\ i_{C_{db}} &= \frac{d}{dt} (C_{db}v_{db} + K_{2C_{db}}v_{db}^2 + K_{3C_{db}}v_{db}^3 + \dots) \end{aligned} \quad (1)$$

Where, the nonlinearity coefficients $K_{2C_{sb}}, K_{3C_{sb}}, \dots, K_{2C_{db}}, K_{3C_{db}}, \dots$ are the derivatives of the currents $i_{C_{sb}}$ and $i_{C_{db}}$ with respect to the voltages v_{sb} and v_{db} .

The drain current i_d depends on all the three terminal voltages, v_{gb} , v_{db} , and v_{sb} . This three dimensional dependencies make the power series of the drain current much more complex than those for the nonlinear capacitors.

The drain current can be described as the power series [8]:

$$i_d = i_d^l + \sum_{k=2}^{\infty} i_d^{nk} \quad (2)$$

Where, i_d^l is the linear component, and i_d^{nk} is the k^{th} -order nonlinear component. In general, the nonlinear components are

$$i_d^{nk} = \sum_{i=0}^k \sum_{j=0}^{k-i} K_{k_{ig,jd,(k-i-j)s}} v_{gb}^i v_{db}^j v_{sb}^{k-i-j} \quad (3)$$

The nonlinearity coefficients K are the partial derivatives of the drain current with respect to the terminal voltages, and can be derived from the device model, as shown in equation (4) [8].

$$K_{k_{ig,jd,(k-i-j)s}} = \frac{\partial^k i_d}{\partial v_{gb}^i \partial v_{db}^j \partial v_{sb}^{k-i-j}} \cdot \frac{1}{i! j! (k-i-j)!} \quad (4)$$

As an example, we presented the formula for the linear, the second order, and third order nonlinear terms:

$$i_d^l = g_{gm}v_{gb} + g_{md}v_{db} - g_{ms}v_{sb} \quad (5)$$

$$i_d^{n2} = K_{2g}v_{gb}^2 + K_{2d}v_{db}^2 - K_{2s}v_{sb}^2 + K_{2g,d}v_{gb}v_{db} + K_{2g,s}v_{gb}v_{sb} + K_{2d,s}v_{db}v_{sb} \quad (6)$$

$$\begin{aligned} i_d^{n3} &= K_{3g}v_{gb}^3 + K_{3d}v_{db}^3 - K_{3s}v_{sb}^3 + K_{3g,d}v_{gb}^2v_{db} + K_{3g,s}v_{gb}^2v_{sb} + K_{3d,s}v_{db}^2v_{sb} \\ &+ K_{3g,2s}v_{gb}v_{sb}^2 + K_{3d,2s}v_{db}v_{sb} + K_{3d,2s}v_{db}v_{sb}^2 + K_{3g,d,s}v_{gb}v_{db}v_{sb} \end{aligned} \quad (7)$$

3.2 MOSFET modeling using operators F , G , and H

We observed that the nonlinear components i_d^{nk} of the drain current i_d can be expressed in a new format by factoring out the common terminal voltages. The factored form is highly regular as it describes MOSFET nonlinearities as compositions of three linear operators, called operators F , G , and H . The next section explains that the proposed factored form (which replaces equations (1)-(3) by equations (13)-(19)) is essential in systematic developing of structural nonlinear macromodels.

Following are the factored representations for the second and third order nonlinear components of drain current i_d :

$$i_d^{n2} = v_{gb}(K_{2g}v_{gb} + K_{2g,d}v_{db} + K_{2g,s}v_{sb}) + v_{db}(K_{2d}v_{db} + K_{2d,s}v_{sb}) + v_{sb}(-K_{2s}v_{sb}) \quad (8)$$

$$\begin{aligned} i_d^{n3} &= v_{gb}(v_{gb}(K_{3g}v_{gb} + K_{3g,d}v_{db} + K_{3g,s}v_{sb}) + v_{db}(K_{3g,d}v_{db} + K_{3g,s}v_{sb}) + v_{sb}(K_{3g,s}v_{sb})) \\ &+ v_{db}(v_{db}(K_{3d}v_{db} + K_{3d,s}v_{sb}) + v_{sb}(K_{3d,s}v_{sb})) + v_{sb}(v_{sb}(-K_{3s}v_{sb})) \end{aligned} \quad (9)$$

Then, $F = K_{2g}v_{gb} + K_{2g,d}v_{db} + K_{2g,s}v_{sb}$; $G = K_{2d}v_{db} + K_{2d,s}v_{sb}$; $H = -K_{2s}v_{sb}$ for the second order nonlinearity, and $F = K_{3g}v_{gb} + K_{3g,d}v_{db} + K_{3g,s}v_{sb}$; $G = K_{3g,d}v_{db} + K_{3g,s}v_{sb}$; $H = K_{3g,s}v_{sb}$, $K_{3d,s}v_{sb}$, $-K_{3s}v_{sb}$ for the third order nonlinearity.

By generalizing for nonlinear components of any order, we introduced the following three linear operators F , G , and H :

$$\begin{cases} F(t_{11}, t_{12}, t_{13}) = t_{11} \cdot v_{gb} + t_{12} \cdot v_{db} + t_{13} \cdot v_{sb} \\ G(t_{22}, t_{23}) = t_{22} \cdot v_{db} + t_{23} \cdot v_{sb} \\ H(t_{33}) = t_{33} \cdot v_{sb} \end{cases} \quad (10)$$

Where, t_{ij} is the coefficient for the terminal voltages.

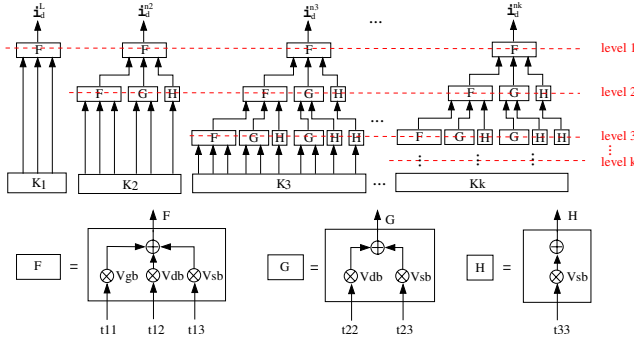


Figure 2: Nonlinear model for drain current of a MOSFET

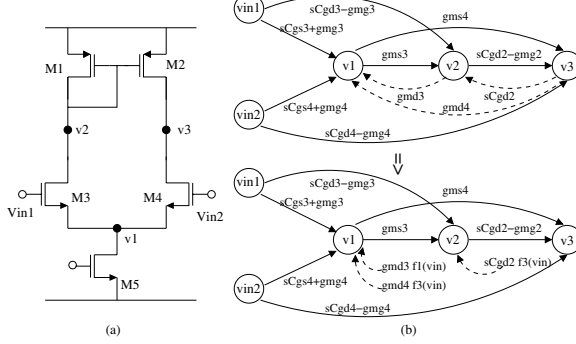


Figure 3: Single-stage OpAmp (a) topology (b) linear model

We showed next that any nonlinear component of the drain current i_d can be expressed as a composition of the three operators.

The k^{th} order nonlinear component of the drain current i_d can be written as:

$$i_d^k = F(f_{(k,1)|F}, g_{(k,1)|F}, h_{(k,1)|F}) \quad (11)$$

Where, $f_{(k,1)|F}$, $g_{(k,1)|F}$, and $h_{(k,1)|F}$ denote the coefficients of operator F at level 1 for the k^{th} order nonlinearity. These coefficients can be further extended as

$$\begin{cases} f_{(k,1)|F} = F(f_{(k,2)|FF}, g_{(k,2)|FF}, h_{(k,2)|FF}) \\ g_{(k,1)|F} = G(g_{(k,2)|FG}, h_{(k,2)|FG}) \\ h_{(k,1)|F} = H(h_{(k,2)|FH}) \end{cases} \quad (12)$$

Where, $f_{(k,2)|FF}$, $g_{(k,2)|FF}$, and $h_{(k,2)|FF}$ are the coefficients of operator F at level 2 for the coefficient $f_{(k,1)|F}$ of level 1. $g_{(k,2)|FG}$ and $h_{(k,2)|FG}$ denote the coefficients of operator G at level 2 for the coefficient $g_{(k,1)|F}$ of level 1. $h_{(k,2)|FH}$ denotes the coefficients of operator H at level 2 for the coefficient $h_{(k,1)|F}$ of level 1.

Similarly, the coefficients at level 2 can be further extended and expressed using the functions from level 3. After $k-1$ steps, the coefficients at level $k-1$ are expressed as functions from level k , whose coefficients are the nonlinearity coefficients K_k derived from the MOSFET device model (equation (4)).

Hence, the general form for the k^{th} nonlinear component of the drain current can be expressed as:

$$\begin{aligned} i_d^k = & F(F \cdots (F(F(K_{k_g}, K_{k_{(k-1)gd}}, K_{k_{(k-1)gs}}) + G(K_{k_{(k-2)gd}}, K_{k_{(k-2)gs}}) \\ & + H(K_{k_{(k-2)gs}})) + \cdots) + \cdots) + G(G \cdots (G(G(K_{k_d}, K_{k_{(k-1)ds}}) \\ & + H(K_{k_{(k-2)ds}})) + \cdots) + \cdots) + H(H \cdots (H(H(-K_{k_s})) \\ & + \cdots) + \cdots) + \cdots) \end{aligned} \quad (13)$$

For example, the second order nonlinear component is

$$i_d^2 = F(f_{(2,1)|F}, g_{(2,1)|F}, h_{(2,1)|F}) \quad (14)$$

Where,

$$\begin{cases} f_{(2,1)|F} = F(f_{(2,2)|FF}, g_{(2,2)|FF}, h_{(2,2)|FF}) = F(K_{2_g}, K_{2_{g,d}}, K_{2_{g,s}}) \\ g_{(2,1)|F} = G(g_{(2,2)|FG}, h_{(2,2)|FG}) = G(K_{2_d}, K_{2_{d,s}}) \\ h_{(2,1)|F} = H(h_{(2,2)|FH}) = H(-K_{2_s}) \end{cases} \quad (15)$$

Similarly, the third order nonlinear component is

$$i_d^3 = F(f_{(3,1)|F}, g_{(3,1)|F}, h_{(3,1)|F}) \quad (16)$$

Where,

$$\begin{cases} f_{(3,1)|F} = F(f_{(3,2)|FF}, g_{(3,2)|FF}, h_{(3,2)|FF}) \\ g_{(3,1)|F} = G(g_{(3,2)|FG}, h_{(3,2)|FG}) \\ h_{(3,1)|F} = H(h_{(3,2)|FH}) \end{cases} \quad (17)$$

and,

$$\begin{cases} f_{(3,2)|FF} = F(f_{(3,3)|FFF}, g_{(3,3)|FFF}, h_{(3,3)|FFF}) = F(K_{3_g}, K_{3_{2g,d}}, K_{3_{2g,s}}) \\ g_{(3,2)|FF} = G(g_{(3,3)|FFG}, h_{(3,3)|FFG}) = G(K_{3_g,2d}, K_{3_{g,d,s}}) \\ h_{(3,2)|FF} = H(h_{(3,3)|FFH}) = H(K_{3_g,2s}) \\ g_{(3,2)|FG} = G(g_{(3,3)|FGG}, h_{(3,3)|FGG}) = G(K_{3_d}, K_{3_{2d,s}}) \\ h_{(3,2)|FG} = H(h_{(3,3)|FGH}) = H(K_{3_{d,2s}}) \\ h_{(3,2)|FH} = H(h_{(3,3)|FHH}) = H(-K_{3_s}) \end{cases} \quad (18)$$

Since the nonlinear capacitors C_{db} and C_{sb} only depend on the voltages v_{db} and v_{sb} , respectively, they can be expressed using only operator H as

$$\begin{aligned} i_{C_{sb}} &= \frac{d}{dt} (C_{sb} v_{sb} + H(H(K_{C_{sb}})) + H(H(H(K_{C_{sb}})))) + \cdots \\ i_{C_{db}} &= \frac{d}{dt} (C_{db} v_{db} + H(H(K_{2C_{db}})) + H(H(H(K_{3C_{db}})))) + \cdots \end{aligned} \quad (19)$$

Figure 2 illustrates the representation of the drain current as composition of operators F , G , and H . In general, the k^{th} order nonlinearity is described by k levels of composition. Operators F , G , and H are linear compositions of the terminal voltages (v_{gb} , v_{db} , v_{sb}) and the outputs from the level below.

4. STRUCTURAL NONLINEAR MODELING

Structural analog circuit macromodeling is difficult because of the strong coupling between the nonlinear devices of the circuit. Macromodeling requires in essence removing the feedback connections in a circuit. In a recent paper [12], a systematic methodology for producing linear structural macromodels is proposed by decoupling of the feedback connections in a circuit. The methodology eliminates the feedback voltage dependencies by equivalent current sources, as shown in Figure 3 (eliminated dependencies are represented in dashed line). Model uncoupling is done in two steps: (1) it defines the decoupling sequence of the blocks by signal path tracing, and (2) the symbolic expression for the equivalent current sources is calculated in the order of the decoupling sequence. The generated macromodels not only give insight into circuit operation, but also significantly reduce the simulation time. For nonlinear circuits, symbolically eliminating the feedback dependencies requires solving a set of nonlinear equations. It is well known that symbolic nonlinear equations of a general form cannot be solved. Therefore, the decoupling of nonlinear circuits cannot be performed exactly (like for linear circuits), and some sort of controlled approximation must be performed.

For nonlinear circuit decoupling, we propose a technique that approximates a nonlinear system of order K by a nonlinear system of order $K-1$ and a correspondingly transformed input. By recursively applying this idea, a nonlinear system is first transformed into a system with linear dependencies of its building blocks, and nonlinear inputs. Then, the resulting linear feedback dependencies are removed by solving linear equations. The decoupling algorithm is based on the representation of MOSFET nonlinearities as compositions of three linear operators F , G , and H , as well as the dependencies between the voltages for each node in the circuit.

Next, we introduced the nonlinear decoupling algorithm based on the previous two properties.

For an analog circuit composed of N nodes and M inputs ($M=1$ or 2), each transistor is replaced by its nonlinear model (Figure 1).

```

% Part I: Nonlinear transformation
k = K; % for Kth order nonlinearity
while k > 1
    for i = 1 : I % I is the total number of nonlinear elements
        ink  $\Rightarrow$  F, G, H(ink);
    end for
    Calculate symbolic  $\mathbf{T}_{G_n^{(k)}}, \mathbf{T}_{C_n^{(k)}}, \mathbf{T}_{G_{in,n}^{(k)}}$ ;
    k = k - 1;
end while
Calculate symbolic  $\sum_k \mathbf{T}_{G_n^{(k)}}, \sum_k \mathbf{T}_{C_n^{(k)}}, \sum_k \mathbf{T}_{G_{in,n}^{(k)}}$ ;
Calculate symbolic  $\mathbf{v}$ ;
% Part II: Model generation
i = 1;
while  $\epsilon > \epsilon$  %  $\epsilon$  is the required accuracy
    i++;
    Calculate  $\sum_k \mathbf{T}_{G_n^{(k)}}, \sum_k \mathbf{T}_{C_n^{(k)}}, \sum_k \mathbf{T}_{G_{in,n}^{(k)}}$ ;
    Calculate  $\mathbf{v}^{[i]}$ ;
    Calculate  $\epsilon = \mathbf{v}^{[i]} - \mathbf{v}^{[i-1]}$ ;
end while

```

Figure 4: Nonlinear decoupling algorithm

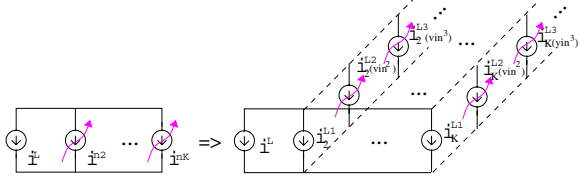


Figure 5: Extensible nonlinear model

Using Kirchhoff's current laws (KCL), the following equation set is set up

$$\begin{aligned} \mathbf{G}_L \mathbf{v} + \sum_{k=2}^K \mathbf{G}_n^{(k)} \mathbf{v}^{(k)} + \frac{d}{dt} \left(\mathbf{C}_L \mathbf{v} + \sum_{k=2}^K \mathbf{C}_n^{(k)} \mathbf{v}^{(k)} \right) \\ = \mathbf{G}_{in,L} \mathbf{v}_{in} + \frac{d}{dt} (\mathbf{C}_{in,n} \mathbf{v}_{in}) + \sum_{k=2}^K \mathbf{G}_{in,n}^{(k)} \mathbf{v}^{(k-1)} \mathbf{v}_{in} \end{aligned} \quad (20)$$

Where, $\mathbf{v} = [v_1(t), v_2(t), \dots, v_N(t)]'$ is a voltage vector, $\mathbf{v}_{in} = [v_{in,1}, \dots, v_{in,M}]'$ are inputs, and $\mathbf{v}^{(k)}$ is the nonlinear voltage vector with elements of the form $\prod_{j=1}^k v_{i_j}$, and $v_{i_j} \in (v_1, \dots, v_N)$. Matrices \mathbf{G}_L and \mathbf{C}_L are the coefficient matrices of the voltage vector due to the linear response of the system by the resistive elements and capacitive elements, respectively.

Matrices $\mathbf{G}_n^{(k)}$ and $\mathbf{C}_n^{(k)}$ denote the impact of the k^{th} order nonlinearity of the resistive elements and capacitive elements on the system, respectively. Matrices $\mathbf{G}_{in,L}$ and $\mathbf{C}_{in,L}$ are the resistive and capacitive linear coefficient matrices of the input vector \mathbf{v}_{in} . $\mathbf{G}_{in,n}^{(k)}$ are the k^{th} order nonlinear coefficients for the inputs.

An example of the above matrices was given in equations (25)–(27) in Section 5.

LEMMA 1. The K^{th} order nonlinear system in equation (20) can be transformed into the following expression

$$\begin{aligned} \left(\mathbf{G}_L + \mathbf{T}_{G_n^{(k)}} \right) \mathbf{v} + \sum_{k=2}^{K-1} \mathbf{G}_n^{(k)} \mathbf{v}^{(k)} + \frac{d}{dt} \left(\left(\mathbf{C}_L + \mathbf{T}_{C_n^{(k)}} \right) \mathbf{v} + \sum_{k=2}^{K-1} \mathbf{C}_n^{(k)} \mathbf{v}^{(k)} \right) \\ = \left(\mathbf{G}_{in,L} + \mathbf{T}_{G_{in,n}^{(k)}} \right) \mathbf{v}_{in} + \frac{d}{dt} (\mathbf{C}_{in,n} \mathbf{v}_{in}) + \sum_{k=2}^{K-1} \mathbf{G}_{in,n}^{(k)} \mathbf{v}^{(k-1)} \mathbf{v}_{in} \end{aligned} \quad (21)$$

Where, $\mathbf{T}_{G_n^{(k)}}, \mathbf{T}_{C_n^{(k)}},$ and $\mathbf{T}_{G_{in,n}^{(k)}}$, called transformation matrices, are linear functions of the node voltages expressed using the three linear composition operators F, G , and H .

As an illustrating example for the lemma, for the single stage OpAmp in Figure 3(a), the above transformation matrix is expressed symbolically as equation (29) (Section 5).

After a sequence of $(K-1)$ steps, equation (20) becomes

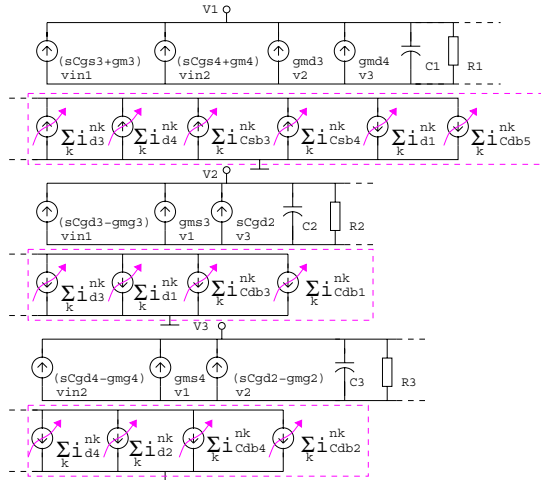


Figure 6: Nonlinear macromodel for single stage OpAmp

$$\begin{aligned} \left(\mathbf{G}_L + \sum_{k=0}^{K-2} \mathbf{T}_{G_n^{(K-k)}} \right) \mathbf{v} + \frac{d}{dt} \left(\left(\mathbf{C}_L + \sum_{k=0}^{K-2} \mathbf{T}_{C_n^{(K-k)}} \right) \mathbf{v} \right) \\ = \left(\mathbf{G}_{in,L} + \sum_{k=0}^{K-2} \mathbf{T}_{G_{in,n}^{(K-k)}} \right) \mathbf{v}_{in} + \frac{d}{dt} (\mathbf{C}_{in,n} \mathbf{v}_{in}) \end{aligned} \quad (22)$$

Where, matrices $\mathbf{T}_{G_n^{(K-k)}}, \mathbf{T}_{C_n^{(K-k)}},$ and $\mathbf{T}_{G_{in,n}^{(K-k)}}$ are the nonlinear symbolic transformation matrices. If the voltage variables in the above matrices are replaced by the symbolic functions of the inputs derived for the linear case (as in [12]) then, the K^{th} order nonlinear system is reduced to a nonlinear system with linear dependencies of the macromodel parameters and nonlinear dependencies of the inputs. This system can be solved to remove the linear feedback dependencies. We denote this solution as $\mathbf{v}^{[1]}$, meaning that it is the solution for the first iteration.

If the above solution does not meet the required modeling accuracy, $\mathbf{v}^{[1]}$ is substituted into the transformation matrices again. In general, at iteration $i+1$, by substituting $\mathbf{v}^{[i]}$, transformation matrices $\mathbf{T}_{G_n^{(K-k)}}, \mathbf{T}_{C_n^{(K-k)}},$ and $\mathbf{T}_{G_{in,n}^{(K-k)}}$ are calculated, and the solution

$\mathbf{v}^{[i+1]}$ for iteration $i+1$ is obtained from equation (22). Hence, by a sequence of substitutions and solvings of linear equations, the solution (and the corresponding macromodel) converges to a fixed point, if the following condition is satisfied:

$$\det \left[\begin{array}{cccccc} \mathbf{e}_1 & \mathbf{e}_2 & \dots & \mathbf{e}_n & \dots & \mathbf{e}_N \end{array} \right] \neq 0 \quad (23)$$

Where, \mathbf{e}_n is the N dimensional vector in equation (24), denoting the difference between the solutions for iterations $i-1$ and i .

$$\sum_{k=0}^{K-2} \frac{\partial \left(\mathbf{T}_{G_n^{(K-k)}} + \frac{d}{dt} \left(\mathbf{T}_{C_n^{(K-k)}} \right) \right)}{\partial v_n} \mathbf{v}^{[i]} - \sum_{k=0}^{K-2} \frac{\partial \left(\mathbf{T}_{G_{in,n}^{(K-k)}} \right)}{\partial v_n} \mathbf{v}_{in} \quad (24)$$

If the determinant of the error matrix is not equal to zero then $\mathbf{0}$ is the only solution of $\mathbf{e} = \mathbf{0}$. Therefore, the solution converges.

The nonlinear decoupling algorithm is summarized in Figure 4. First of all, the symbolic expressions for matrices $\mathbf{T}_{G_n^{(k)}}, \mathbf{T}_{C_n^{(k)}},$ and $\mathbf{T}_{G_{in,n}^{(k)}}$ are derived by applying the transformation (21) for transforming the system from an order k to order $k-1$ through using the three operators F, G , and H . Then, the symbolic expression for voltage \mathbf{v} is derived from equation (22), as shown in Part I of the algorithm. Then, the symbolic expression $\mathbf{v}^{[i]}$ is iteratively substituted into matrices $\mathbf{T}_{G_n^{(k)}}, \mathbf{T}_{C_n^{(k)}},$ and $\mathbf{T}_{G_{in,n}^{(k)}}$ to calculate $\mathbf{v}^{[i+1]}$, until the required accuracy is met, as shown in Part II of the algorithm.

Figure 5 shows an example of the equivalent model capturing up to the K^{th} order nonlinearities. Each nonlinearity is replaced by several equivalent current sources, which are nonlinear functions of the input voltages. The number of the extension stages of the current sources is determined by the required modeling accuracy.

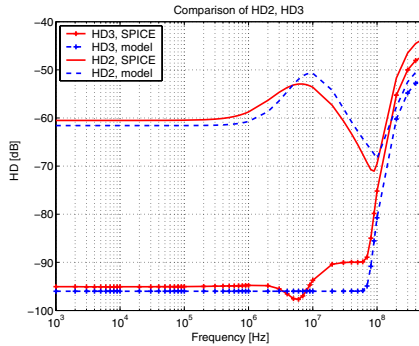


Figure 7: HD2 and HD3 for SPICE and macromodel

5. CASE STUDIES FOR NONLINEAR MODEL

5.1 Single-stage OpAmp

Figure 3(a) shows the topology of a single-stage OpAmp. We used the modeling of the second order nonlinearity as an example to explain how the proposed nonlinear decoupling algorithm is used.

If only the second order nonlinearity is considered, the circuit is described by the following equation

$$\left(\mathbf{G}_L + \mathbf{T}_{\mathbf{C}_n^{(2)}} \right) \mathbf{v} + \frac{d}{dt} \left(\left(\mathbf{C}_L + \mathbf{T}_{\mathbf{C}_n^{(2)}} \right) \mathbf{v} \right) = \left(\mathbf{G}_{in,L} + \mathbf{T}_{\mathbf{G}_{in,n}^{(2)}} \right) \mathbf{v}_{in} + \frac{d}{dt} \left(\mathbf{C}_{in,n} \mathbf{v}_{in} \right) \quad (25)$$

Where,

$$\mathbf{G}_L = \begin{pmatrix} -G_1 & g_{md3} & g_{md4} \\ g_{ms3} & -G_2 & 0 \\ g_{ms4} & -g_{mg2} & -G_3 \end{pmatrix}, \quad \mathbf{C}_L = \begin{pmatrix} -C_1 & 0 & 0 \\ 0 & -C_2 & C_{gd3} \\ 0 & C_{gd2} & -C_3 \end{pmatrix} \quad (26)$$

$$\mathbf{G}_{in,L} = \begin{pmatrix} -g_{mg3} & -g_{mg4} \\ g_{mg3} & 0 \\ 0 & g_{mg4} \end{pmatrix}, \quad \mathbf{C}_{in,L} = \begin{pmatrix} -C_{gs3} & -C_{gs4} \\ -C_{gd3} & 0 \\ 0 & -C_{gd4} \end{pmatrix} \quad (27)$$

In which,

$$\begin{cases} G_1 = g_{ms3} + g_{ms4} + g_{md5} \\ G_2 = g_{md3} + g_{mg1} + g_{md1} \\ G_3 = g_{md4} + g_{md2} \\ C_1 = C_{gs3} + C_{sb3} + C_{gs4} + C_{sb4} + C_{db5} + C_{gd5} \\ C_2 = C_{gd3} + C_{db3} + C_{gs1} + C_{gb1} + C_{db1} + C_{gs2} + C_{gd2} + C_{db2} \\ C_3 = C_{gd4} + C_{db4} + C_{gd2} + C_{db2} \end{cases} \quad (28)$$

If we use symbols f , g , and h to denote $f_{(2,1)|F}$, $g_{(2,1)|F}$, and $h_{(2,1)|F}$ in equation (14), respectively, then

$$\mathbf{T}_{\mathbf{G}_n^{(2)}} = \begin{pmatrix} h_3 + h_4 - h_5 & g_3 & g_4 \\ -h_3 & -f_1 - g_1 - g_3 & 0 \\ -h_1 & 0 & -g_4 - f_2 - g_2 \end{pmatrix}$$

$$\mathbf{T}_{\mathbf{C}_n^{(2)}} = \begin{pmatrix} -(K_2 C_{sb3} + K_2 C_{db5}) v_1 \\ -(K_2 C_{db3} + K_2 C_{db1}) v_2 \\ -(K_2 C_{db4} + K_2 C_{db2}) v_3 \end{pmatrix} \cdot I_{3 \times 3}, \quad \mathbf{T}_{\mathbf{G}_{in,n}^{(2)}} = - \begin{pmatrix} f_3 & f_4 \\ f_3 & 0 \\ 0 & f_4 \end{pmatrix} \quad (29)$$

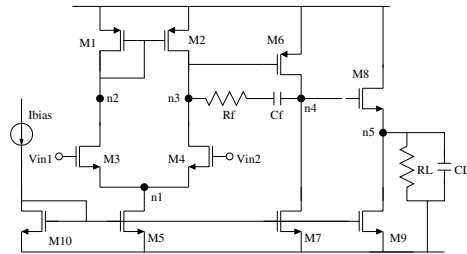
Please note that symbols f , g , and h are linear function of the node voltages. For example,

$$f_3 = f_{3(2,1)|F} = F(K_{2,g,3}, K_{2,gd,3}, K_{2,gs,3}) = K_{2,g,3} v_{in1} + K_{2,gd,3} v_2 + K_{2,gs,3} v_1 \quad (30)$$

Then, voltages (v_1, v_2, v_3) in the matrices $\mathbf{T}_{\mathbf{G}_n^{(2)}}$, $\mathbf{T}_{\mathbf{C}_n^{(2)}}$, and $\mathbf{T}_{\mathbf{G}_{in,n}^{(2)}}$ are replaced by the voltages derived from the linear circuit $(v_1^{[1]}, v_2^{[1]}, v_3^{[1]})$. The above matrices become $\mathbf{T}_{\mathbf{G}_n^{(1)}}$, $\mathbf{T}_{\mathbf{C}_n^{(1)}}$, and $\mathbf{T}_{\mathbf{G}_{in,n}^{(1)}}$.

This step removes the nonlinear dependencies between the node voltages. The nonlinear terms only come from the functions of the inputs, which are known. In the frequency domain, equation (25) becomes

$$\left(\mathbf{G}_L + \mathbf{T}_{\mathbf{G}_n^{(1)}} + s \left(\mathbf{C}_L + \mathbf{T}_{\mathbf{C}_n^{(1)}} \right) \right) \mathbf{V} = \left(\mathbf{G}_{in,L} + \mathbf{T}_{\mathbf{G}_{in,n}^{(1)}} + s \mathbf{C}_{in,n} \right) \mathbf{V}_{in} \quad (31)$$



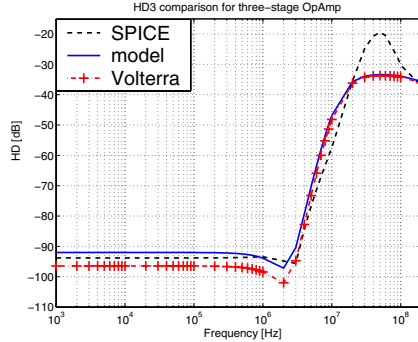


Figure 11: HD3 for SPICE, Volterra series, and macromodel

frequencies. For third order harmonic distortion, both curves increase dramatically beyond $60MHz$. The modeling error is small, being below $6dB$ for the frequency range from $1kHz$ to $500MHz$.

The convergency condition of the nonlinear decoupling algorithm was checked by substituting matrix (31) into the error matrix (24). For the considered set of transistor dimensions, the determinant of the error matrix converged to a none-zero number, which means that the accuracy of the macromodel converges to a fixed point by extending the equivalent nonlinear current sources.

Figure 12 presents the dependency of the accuracy of the nonlinear macromodel with respect to the complexity of the model. For frequencies up to $10MHz$, the error of the model is reduced from 10% to 4.5% by using a second iteration to insert more nonlinear current sources. Using more iterations, the modeling error is reduced to 3%. The modeling error increases for higher frequency, as shown in solid curve.

5.2 Two-stage OpAmp

Figure 8 shows the topology for a two-stage OpAmp. Figure 9 is the generated nonlinear macromodel. The simulations showed that the produced macromodel is much faster than the SPICE simulation of the original circuit. For example, our model needs less than 1 second in order to calculate third order harmonic distortion from $1kHz$ to $500MHz$, while SPICE simulation of the original circuit takes about 2 minutes.

Figure 10 shows the contribution of the second order harmonic distortion of each transistor. The solid curve is the total HD2 considering all the nonlinearities of all transistors. It is about $-63dB$ for low frequencies, and increases up to $-28dB$ at $10MHz$. As opposed to blackbox models, the produced macromodel gives insight into the circuit operation. For example, the distortion caused by transistor M8, shown as a dashed line, is much larger than that caused by the other transistors (which means that it dominates the total distortion). The distortion caused by one of the current sources M5 is extremely small (below $-200dB$). This means that the nonlinearities of the current sources have very little impact on the linearity of the circuit.

Figure 11 presents the comparison for the third order harmonic distortion obtained through our macromodel (dashed curve), Volterra series analysis (dashed curve with plus marker), and SPICE simulation of the original circuit (solid curve). It shows that our macromodeling method has similar accuracy as Volterra series analysis. It also has good agreement with SPICE simulation for low to medium-high frequencies. However, the prediction of the nonlinear behavior at high frequencies is worse, due to the neglecting of some nonlinear sources for the MOSFET transistor. More nonlinear elements ought to be considered in Figure 1 to achieve better accuracy at high frequencies.

Figure 12 presents the accuracy of the model for different num-

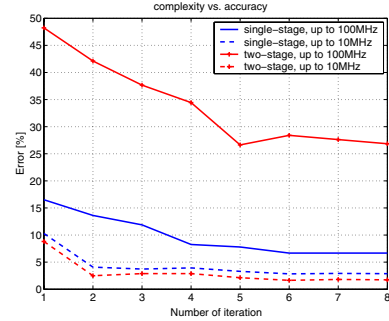


Figure 12: Macromodel accuracy vs. complexity

ber of iterations in the nonlinear decoupling algorithm. For frequencies up to $10MHz$, an error of 3% can be achieved by using three iterations. The improvement of accuracy is not significant (about 1%) by using more stages for the equivalent nonlinear sources. For higher frequencies, as shown in the solid curve with plus marker, the modeling error becomes large, e.g., the macromodel fails capturing the increase in HD2 between $20MHz$ and $100MHz$, as shown in Figure 11. For that frequency range, HD3 is around $-34dB$ for our model and larger ($-20dB$) for SPICE simulation of the original circuit. However, at that frequency, the circuit stopped to operate properly, and therefore, the modeling error of the macromodel is not as critical as for a well-behaved circuit.

6. CONCLUSION

This paper presents a systematic methodology to automatically generate structural nonlinear macromodels customized for a specific analog circuit. The idea is to approximate a nonlinear system as a system with nonlinear inputs and linear dependencies of its composing blocks. The novel contributions include (1) regular description of circuit nonlinearities based on three operators F, G, H, (2) a nonlinear decoupling algorithm to approximate nonlinear dependencies by linear dependencies with nonlinear transformation of the inputs, and (3) an iterative algorithm to create macromodels. The produced models are symbolic, and are extendable to incorporate more stages according to the required accuracy. Experiments are offered for two OpAmp circuits. Produced models offer insight into the circuit, and good accuracy compared to SPICE.

7. REFERENCES

- [1] N. Dong, and J. Roychowdhury, "Piecewise Polynomial Nonlinear Model Reduction", *Proc. of DAC*, pp. 484–489, 2003.
- [2] P. Li, and L. T. Pileggi, "Compact Reduced-Order Modeling of Weakly Nonlinear Analog and RF Circuits", *IEEE Trans. CAD*, Feb 2005.
- [3] P. Li, and L. T. Pileggi, "Efficient Per-Nonlinearity Distortion Analysis for Analog and RF Circuits", *IEEE Trans. CAD*, Oct 2003.
- [4] M. Storace, O. D. Feo, "Piecewise-Linear Approximation of Nonlinear Dynamical Systems", *IEEE Trans. C&S I*, Apr 2004.
- [5] X. Huang *et al.*, "Modeling Nonlinear Dynamics in Analog Circuits via Root Localization", *IEEE Trans. CAD*, pp. 895–907, Jul. 2003.
- [6] P. Wambacq, G. Gielen, P. Kinget, and W. Sansen, "High-Frequency Distortion Analysis of Analog Integrated Circuits", *IEEE Trans. C&S II*, Mar 1999.
- [7] P. Dobrovolny *et al.*, "Analysis and Compact Behavioral Modeling of Nonlinear Distortion in Analog Communication Circuits", *IEEE Trans. CAD*, VOL. 22, NO. 9, pp. 1215–1227, Sept 2003.
- [8] Piet Wambacq, Willy M.C. Sansen, Distortion Analysis of Analog Integrated Circuits. *Kluwer Academic Publishers*. 1998.
- [9] A. Buonomo, and A. L. Schiavo, "Perturbation Analysis of Nonlinear Distortion in Analog Integrated Circuits", *IEEE Trans. C&S I*, Aug 2005.
- [10] J. R. Phillips, "Projection-Based Approaches for Model Reduction of Weakly Nonlinear, Time-Varying Systems", *IEEE Trans. CAD*, Feb 2003.
- [11] M. Rewienski, "A Trajectory Piecewise-Linear Approach to Model Order Reduction of Nonlinear Dynamical Systems", MIT. 2003.
- [12] Y. Wei, A. Doboli, "Systematic Development of Analog Circuit Structural Macromodels through Behavioral Model Decoupling", *Proc. of DAC*, 2005.